Journal of
Materials Chemistry C

Accepted Manuscript

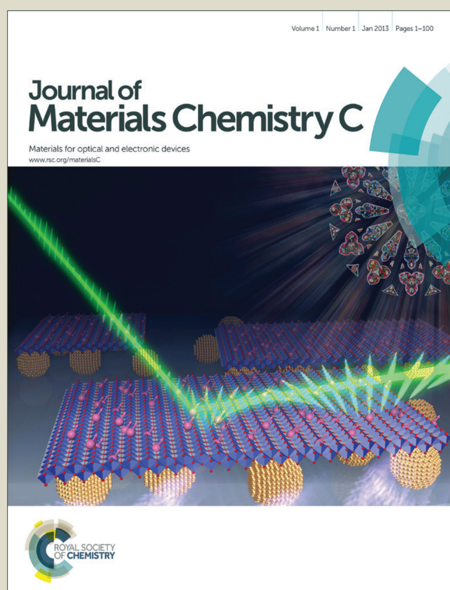

This is an *Accepted Manuscript*, which has been through the Royal Society of Chemistry peer review process and has been accepted for publication.

Accepted Manuscripts are published online shortly after acceptance, before technical editing, formatting and proof reading. Using this free service, authors can make their results available to the community, in citable form, before we publish the edited article. We will replace this *Accepted Manuscript* with the edited and formatted *Advance Article* as soon as it is available.

You can find more information about *Accepted Manuscripts* in the Information for Authors.

Please note that technical editing may introduce minor changes to the text and/or graphics, which may alter content. The journal's standard Terms & Conditions and the Ethical guidelines still apply. In no event shall the Royal Society of Chemistry be held responsible for any errors or omissions in this *Accepted Manuscript* or any consequences arising from the use of any information it contains.

ROYAL SOCIETY OF CHEMISTRY

www.rsc.org/materialsC

Production of centimeter-scale sub-wavelength nanopatterns by controlling the light path of adhesive photomask

Jin Wu[a], Kai Tao[a] and Jianmin Miao*[a]

[a]School of Mechanical and Aerospace Engineering, Nanyang Technological University, 50

Nanyang Avenue, Singapore 639798.

Email: MJMMiao@ntu.edu.sg

Journal of Materials Chemistry C Accepted Manuscript

Abstract

The capability of generating sub-wavelength nanostructures in a low-cost and high yield fashion is important for many areas of research. In this work, a facile parallel near-field photolithography strategy was developed to enable centimeter-scale nanopatterns with sub-wavelength feature size and variable feature shapes by utilizing metal coating to manipulate the light path of polydimethylsiloxane (PDMS) structure based photomasks. The thin metal coating and microscale apertures created on PDMS structures not only imparted the adhesive and conformal merits to the elastomeric photomasks, but also be capable of making the nanoscale regions below V-shape PDMS tips apexes or vertical sidewalls of flat PDMS reliefs be selectively exposed by controlling the light path. Thus, sub-100 nm nanostructures were generated over large areas on substrate. For the first time, two under exposures in near-field photolithography were employed to fabricate sub-wavelength nanorod array with adjustable ratio of length to width by rotating photomask in the second exposure. Besides generation of the smallest 70 nm photoresist features and 80 nm metal nanostructures, this technique was also exploited to fabricate self-assembled monolayers (SAMs) molecular nanopatterns with sub-wavelength feature size. This nanolithography strategy combines the advantages of low-cost, high productivity, sub-wavelength feature size and flexible feature geometries, making it a facile and general nanofabrication tool to enable various functional nanostructures for academic research.

Keywords: photolithography, sub-wavelength nanostructures, PDMS tip array, nanorod, molecular nanopatterns

Journal of Materials Chemistry C Accepted Manuscript

Introduction

In recent years, sub-wavelength nanostructures have been extensively explored for widespread applications in many fields, including plasmonics, photonics, photovoltaics, biological/chemical sensors and cell-material interactions.[1-6] Development of increasingly complex and miniaturized devices prompts the exploration for scalable, low-cost, high-resolution and ease-of-use lithography systems.[7-13] Although various top-down nanofabrication methods such as photolithography,[11, 12, 14-19] electron beam lithography (EBL),[20, 21] nanoimprint lithography,[22, 23] and scanning probe based lithography (SPL),[24-31] have been developed to define materials at nanoscale size with good registration, and many bottom-up lithographic approaches such as block copolymer lithography,[32, 33] nanosphere lithography[34-36] and electrically induced pattern formation[37-40] are exploited to fabricate nanostructures with high resolution, the achievement of sub-wavelength, uniform and highly ordered nanostructures over large areas in a simple and cost-effective fashion remains challenging.[1, 7, 8] Amongst the lithographic strategies, photolithography is the mainstay for production of micro/nanoscale structures owing to its high productivity, well-established protocols and implementation in semiconductor device manufacturing.[12, 28, 41] In conventional photolithography, the rigid substrates such as fused quartz and high-purity glass covered with micrometer-sized opaque metals are exploited as photomasks to replicate patterns with microscale feature size.[11, 42] However, the far field light diffraction is inevitable because the intimate contact between the rigid photomask surface and underlying photoresist surface is hard to achieve, although pressure and vacuum can be employed to reduce the air gap between the two rigid surfaces.[11, 43] The air gap not only results in light diffraction, but also leads to the non-uniform effective exposure dose across substrate surface.[11, 44] To achieve sub-wavelength features by bypassing the far-field light diffraction, utilization of soft and elastomeric materials such as polydimethylsiloxane (PDMS) as photomasks is a good choice,

Journal of Materials Chemistry C Accepted Manuscript

as in the cases of optical soft lithography[11, 15, 18, 45] and beam pen lithography (BPL).[1, 4, 8, 28, 46] Since PDMS structures ensure the intimate and conformal contact with photoresist surfaces, near-field proximity optical effect produces and sub-wavelength nanopatterns are enabled.[8, 11, 18, 47] Compared to conventional hard photomasks, the soft photomasks are not only nondestructive to sample surfaces, but also enable nanopatterning on flexible and curved substrate surfaces.[48, 49]

In optical soft lithography, proper depth of surface reliefs causes the phase shift of odd multiple of π, producing near zero light intensity at every phase edge in the near field of PDMS reliefs.[18, 45, 48] However, it was largely utilized to produce raised positive photoresist nanostructures below the edges of PDMS reliefs, since most of photoresist was exposed due to the transparency nature of PDMS.[11, 14, 18, 47, 50] In contrast, BPL utilized an opaque metal coating to block the transmission of incident light from all areas except nanoscopic apertures created at the apexes of PDMS tips, leading to the exposure of underlying photoresist at nanoscale regions.[8] BPL is advantageous in creating arbitrarily shaped sub-wavelength nanopatterns without designing new photomasks. Nevertheless, the creation of uniform nanoscopic apertures is required, but challenging. Because the procedures are complicated and the aperture size is particularly difficult to control (especially at sub-wavelength size).[28] Ideally, if the tip array with aperture-free or micro-scale apertures could function as well as the tips with nanoscopic apertures, the photomasks fabrication process could be substantially simplified. Thereby the implementation of parallel near-field photolithography could be much easier.

Herein, by coating PDMS structures with a thin layer of opaque metal or creating microscale large apertures at metal-coated PDMS tip array, the adhesive characteristic of PDMS structures was retained and therefore the intimate contact between PDMS protrusions and underlying substrates was ensured over large areas.[51, 52] More importantly, the light path of PDMS structures

Journal of Materials Chemistry C Accepted Manuscript

was modified by the metal coating. Thus, the incident light was only allowed to selectively expose underlying substrate at nanoscale regions. For thin metal coated V-shape PDMS tips without apertures (Figure 1a) and metal-coated V-shape PDMS tips with microscale large apertures (Figure 1b), the incident light was only allowed to pass from tips apexes to selectively expose underlying surface completely. For thin metal coated PDMS flat reliefs (Figure 1c), the incident light was only allowed to pass from the sidewalls of flat reliefs to expose underlying substrates selectively. Consequently, centimeter-scale sub-wavelength nanostructures were realized in near-field photolithography by exploiting three different PDMS structures based photomasks. Since the PDMS photomasks were placed on photoresist coated substrates manually for photolithography, the tip apexes deformation could be minimized due to free of pressure, which benefited in reducing both the effective light spot size and produced feature size. Hence, the smallest feature size of 70 nm was achieved. Besides sub-wavelength photoresist and metal nanostructures, sub-wavelength molecular nanopatterns were also enabled by this nanolithographic method.

Experimental Section

Fabrication of silicon molds of V-shape PDMS tip array. Shipley1805 (MicroChem) photoresist was spin-coated on Si/SiO_2 (100) wafers with the SiO_2 layer thickness of 260 nm. Conventional photolithography was performed on the mask aligner (SUSS MJB4 UV400 from SUSS MicroTec company). Traditional chrome based hard photomasks were used to fabricate microscale features with various feature shapes on Si/SiO_2 wafers. Subsequently, the photoresist patterned Si/SiO_2 wafers were subjected to buffered oxide etch (BOE) (NH_4F:HF = 7:1, v/v) (Transene Company) to remove the 260 nm thick SiO_2 layer inside the exposed photoresist

Journal of Materials Chemistry C Accepted Manuscript

Journal of Materials Chemistry C Accepted Manuscript

features. After removing the photoresist by rinsing the samples in acetone, the patterned wafers were placed in KOH etching solution (30% KOH in H_2O:isopropanol (4:1 v/v)) at 75 ˚C for several minutes with vigorous stirring. The exposed silicon surface inside the features was etched anisotropically, generating V-shape recessed trench profile in vertical direction. Large initial feature sizes required longer etching time to get sub-100 nm apexes at the bottom of V-shape trenches. For example, the initial feature sizes of 1 and 2 and 3 μm demanded the etching time of 2, 4 and 7 min respectively to get sub-100 nm apexes. Noticeably, the apexes sizes of V-shape silicon trenches could be adjusted by controlling the etching time. For example, for the initial feature sizes of 1, 2 and 3 μm on hard photomasks, the etching time of 1.5 min produced the apexes sizes of 30 ± 8 nm, 480 ± 33 nm and 1.3 ± 0.14 μm at the bottom of V-shape silicon trenches respectively. Hence, by controlling the etching time and initial feature size, the apex size of V-shape trench could be adjusted. The V-shape Si trenches could have various shapes horizontally, such as rectangular, square, circle, ladder and miniaturized letters, as determined by the initial feature shapes on hard chrome photomasks. But all Si trenches exhibited V-shape morphology in vertical direction after KOH anisotropical etching. The remaining SiO_2 was removed by placing the samples in BOE for 4 min. Finally, the silicon molds were modified with 1H,1H,2H,2H-perfluorodecyltrichlorosilane (Gelest, Inc.) by gas phase silanization to prevent the adhesion between PDMS and silicon molds during separation.

Fabrication of silicon molds of PDMS flat reliefs. Conventional photolithography was employed to fabricate microscale photoresist patterns on Si/SiO_2 (100) wafers with the SiO_2 layer thickness of 2 μm. The photoresist patterned wafers were subjected to DRIE (deep reactive ion etching) to remove the 2 μm thick SiO_2 layer inside the photoresist features. As such, recessed features with vertical sidewalls were formed. Subsequently after removal of photoresist

by sonication of the samples in acetone, the Si/SiO_2 molds with the trench depth of 2 μm were modified with 1H,1H,2H,2H-perfluorodecyltrichlorosilane (Gelest, Inc.) by gas phase silanization.

Fabrication of PDMS adhesive photomasks. Soft PDMS was used to make adhesive photomasks because of its good sticky property. The liquid PDMS elastomer and cross-linker (Sylgard 184, Dow Corning) were mixed in a 10:1 ratio (w/w). The mixture was stirred, degassed, and then casted on above obtained Si molds with the elastomer thickness of 4 mm. After curing thermally at 70 ℃ for 2 h, the elastomer was carefully separated from the silicon molds and contained the inverse of original pattern geometries on Si molds. As such, transparent V-shape PDMS tip array and flat PDMS reliefs were generated. To fabricate thin metal coated adhesive PDMS photomasks, 20 nm thick gold was coated on the above obtained PDMS structures using electron beam evaporation. For preparation of V-shape metal-coated PDMS tips with nanoscopic or microscale apertures, 60 nm thick Au was coated on the V-shape PDMS tip array. Subsequently, poly(methyl methacrylate) (PMMA) (495 c7, MicroChem Inc., USA) was spin-coated on the 60 nm Au coated V-shape PDMS tips to cover the whole tips surface (1000 rpm for 30 s) and followed by baking of the samples on hot plate at 100 ℃ for 5 min. Oxygen plasma with the oxygen flow of 300 millitorrs in a plasma cleaner (Plasma Cleaner, PDC-32G, Harrick) was employed to etch away the top PMMA layer until the gold coating at the apexes of tips was exposed. Subsequently, the samples were placed in gold etching solution (Gold Etchant TFA:H_2O (1:40, v/v)) to etch away the exposed gold layer at the tips apexes selectively (Typically 3 min). The generated aperture size could be controlled by adjusting oxygen plasma etching time. For example, 90 nm, 300 nm and 1.9 μm wide apertures were obtained by

Journal of Materials Chemistry C Accepted Manuscript

employing the oxygen plasma etching for 8, 10 and 20 min respectively. Finally, the remaining PMMA on the PDMS tips was removed by rinsing the samples in acetone.

Sub-wavelength photolithography with adhesive PDMS photomasks on positive photoresist. The Shipley1805 (MicroChem) positive photoresist was pre-diluted with propylene glycol monomethyl ether acetate (Sigma-Aldrich) at 20% (v/v), 40% (v/v) and 50% (v/v). The 20%, 40% and 50% diluted photoresist was spin-coated on Si/SiO_2 (100) wafers surfaces at 3000 rpm for 30 s to obtain 40, 100 and 130 nm thick photoresist layers respectively. After the photoresist-coated substrates were baked on hot plate at 110 ℃ for 5 min, the samples were used for near-field photolithography. The adhesive photomasks were placed in intimate contact with photoresist coated Si wafers manually. After the adhesive PDMS photomasks were pressed to contact with underlying photoresist coated silicon wafers intimately using tweezer, the soft photomasks would not separate with photoresist during exposure. A halogen light source (Fiber-lite Illuminators MI150, Dolan-Jenner) with adjustable exposure energy from 0 to 250 mW/cm^2 was used to expose underlying photoresist through the adhesive photomasks. The typical exposure time was 2 s. For the V-shape PDMS tips based photomasks in Figure 1a-b, the exposure energy of 250 mW/cm^2 was utilized. For production of nanorod array using two under exposures on 130 nm thick positive photoresist surface, the exposure energy of 105 mW/cm^2 was employed in each exposure. For production of grid photoresist array using two exposures on 40 nm thick positive photoresist surface, the exposure energy of 250 mW/cm^2 was employed in each exposure. For the PDMS flat relief based photomasks in Figure 1c, the exposure energy of 150 mW/cm^2 was employed. After exposure, the photoresist was developed in a MF319 developer (MicroChem) for 30 s. To fabricate metal nanopatterns, 12 nm Cr or 2 nm Cr/10 nm Au was coated on the obtained photoresist patterns by electron beam evaporation, followed by placing

Journal of Materials Chemistry C Accepted Manuscript

the samples in Remove PG (MicroChem Inc., USA) overnight. Finally, the samples were put in Remove PG and acetone under sonication for 1 min in turn to lift off the photoresist, allowing us to visualize the metal nanopattterns by SEM (JEOL JSM-7600), atomic force microscope (AFM) (Park Systems Co.) and optical microscope (Olympus).

Sub-wavelength molecular nanopatterns produced by adhesive PDMS photomasks

20 nm thick Au coated Si wafers were immersed in the ethanol (HPLC purity, Sigma-Aldrich) solution of dodecanethiol ($HS(CH_2)_{11}CH_3$) for 5 h to form closely packed self-assembled monolayers (SAMs). Before exposure, the samples were rinsed in ethanol for 2 min, and blown dry with nitrogen. After the 20 nm Au coated V-shape PDMS tip array (Figure 1a) was placed on SAMs coated gold substrates, the halogen light source with the exposure energy of 250 mW/cm^2 was deployed to expose the SAMs through adhesive photomask with controlled exposure time, for example, 1, 5, 10 and 20 min. After exposure, AFM was utilized to obtain non-contact phase images of molecular nanopatterns.

Results and Discussion

Sub-Wavelength Photolithography with Thin Metal Coated V-shape PDMS Tip Array

As shown in Figure 1a, the incident light has three different paths toward photoresist surface when it propagates through a V-shape transparent PDMS tip: 1) light that is directed to the contact area of tip apex, 2) light that is incident on the oblique sidewalls of tip, 3) light that incident on the flat backing parts between tips. In this work, we need to make the exposure process dominate by the incident light through path 1). As such, the underlying photoresist below the tip apex can be selectively exposed, producing sub-100 nm nanopatterns. For the light path 2), the total internal reflection at the interface between PDMS and air makes the incident light

Journal of Materials Chemistry C Accepted Manuscript

difficult to pass from these regions.[11, 14, 15] For the light path 3), the incident light may transmit from the flat backing parts to expose underlying photoresist if without modification. To avoid the undesirable exposure through light path 3), a thin layer of opaque gold (20 nm thick) was coated on the surface of PDMS tips to block the transmission of incident light from these regions. It is reported that the effective exposure dose below the contact areas is larger than that beneath the flat baking parts between V-shape PDMS tips.[11, 15] The thin opaque metal layer can block the transmission of incident light from the flat backing parts effectively, but allow incident light to partially pass from the contact areas at tip apexes to expose underlying photoresist selectively, producing sub-wavelength nanostructures. Importantly, the thin metal coating on PDMS tips makes them reserve the adhesive and elastomeric merits of PDMS, which ensures the intimate contact between adhesive PDMS protrution and underlying photoresist surface over large areas without requiring the application of external force during exposure (Figure 1d). The intimate contact enables parallel near-field optical lithography and the generation of sub-wavelength nanostructures (Figure 1a and d).

Journal of Materials Chemistry C Accepted Manuscript

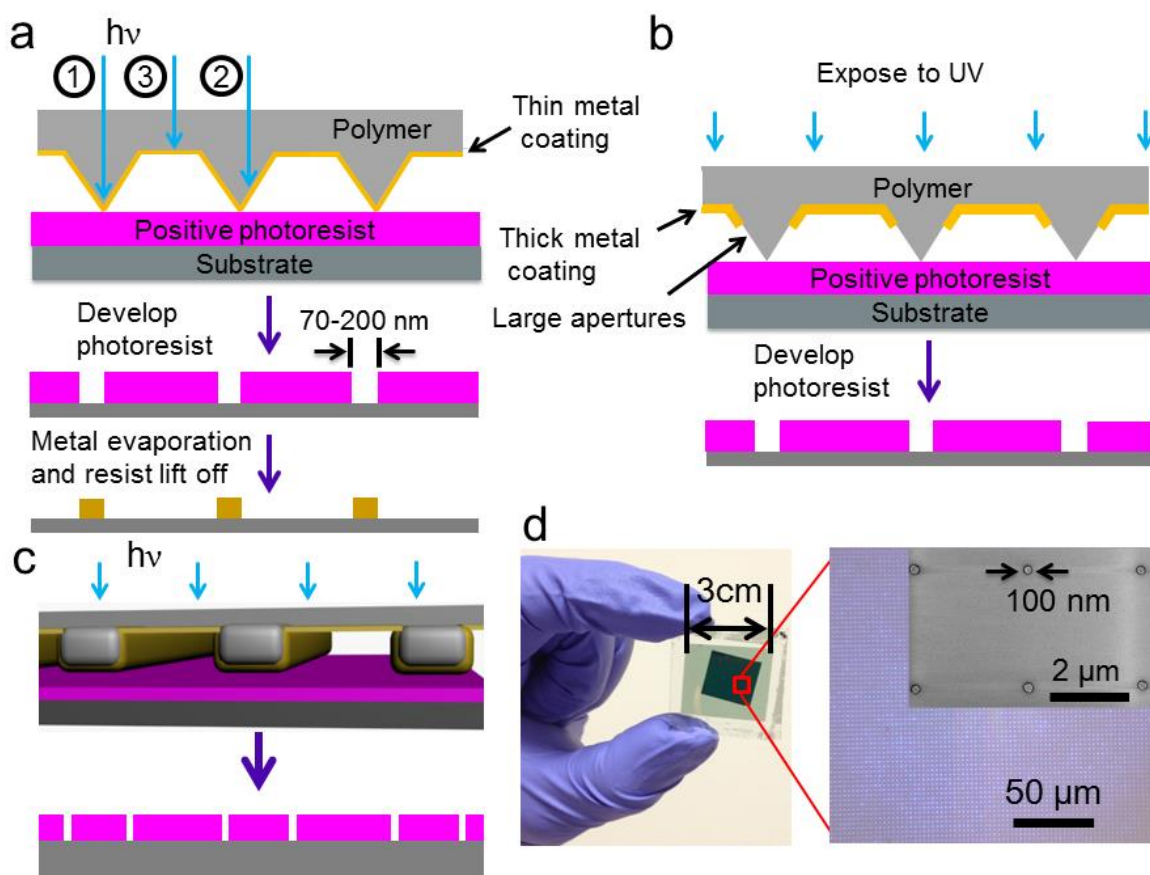

Figure 1. Centimeter-scale sub-wavelength near-field photolithography using metal coating to control the light path of adhesive photomasks. (a) Schematic illustration of sub-wavelength photolithography with thin metal coated V-shape PDMS tip array without apertures. ①, ②and ③ illustrated the light paths towards the contact areas at tips apexes, the oblique sidewalls of tips and the flat backing parts between tips respectively. (b) Scheme illustrating photolithography using V-shape metal coated PDMS tips with large apertures at tips apexes to produce sub-wavelength nanostructures. (c) Schematic showing sub-wavelength photolithography using thin metal coated PDMS flat reliefs. (d) Centimeter-scale sub-wavelength nanopatterns generated by the photomask in (a). The left optical image showed that the photoresist coated silicon wafer was firmly adhered to adhesive photomask without falling off when taking away the mask from the

Journal of Materials Chemistry C Accepted Manuscript

desk without holding the silicon wafer. The right was large-area optical image and corresponding SEM image (Inset) of fabricated 100 nm gold dot array respectively.

The silicon molds with V-shape recessed trench profile in vertical direction were fabricated by combining traditional photolithography with KOH anisotropic wet etching process. The V-shape PDMS tip array with sub-100 nm tips apexes could then be replicated from these silicon molds accordingly (Figure 2a-d). For photolithography with 20 nm thick Au coated V-shape PDMS tip array, only the positive photoresist below the tips apexes was completely exposed when the exposure dose was low (exposure time: 2 s) (Figure S1a). As the exposure dose increased, the photoresist below the flat backing parts was gradually exposed (Figure S1b). When the exposure dose was high enough, all the photoresist was exposed except that below the oblique sidewalls (Figure S1c). It demonstrated that the order of exposure dose through the three different paths followed: 1) > 3) > 2). Besides, the order of measured absorption spectrums for different PDMS configurations followed: transparent V-shape PDMS tip array < 20 nm Au coated flat PDMS slide < 20 nm Au coated V-shape PDMS tip array < 60 nm Au coated V-shape PDMS tip array (Figure 2e). Thus, it confirmed that the incident light towards the sidewalls of V-shape PDMS tips (path 2) was blocked, which could be ascribed to the total internal reflection effect.[14, 28] The UV-vis optical density spectras showed that there was still transmittance through 20 nm Au coated V-shape PDMS tip array in UV region, although 20 nm thick gold coating could block the incident light in part (Figure 2e). Thus, it demonstrated that the exposure process could be dominated by the incident light through path 1) via controlling the exposure dose.

When the adhesive photomask was brought in intimate contact with photoresist coated substrate manually, the substrate surface stuck to the adhesive photomask firmly. The photoresist coated substrate surface did not separate from the adhesive photomask even if the photomask

Journal of Materials Chemistry C Accepted Manuscript

was taken away from the desk without holding the photoresist coated substrate (Figure 1d). Such kind of intimate contact over several square centimeter-scale areas was attributed to the Van der Waals' interaction between the two surfaces.[11, 51] By illuminating vertical incident light through the 20 nm Au coated V-shape PDMS tips for exposure, 100 nm photoresist nanostructures were produced over the areas of 2 × 1.5 cm^2 (Figure 2f). According to the analysis of feature size uniformity at 10 different places across the areas of 2 × 1.5 cm^2, the uniformity was 10 %, indicating that uniform nanopatterns across large areas could be realized by the adhesive photomasks (Figure S2). Since the backside of elastomeric photomasks was free of external pressure and the tips remained intact, the size of contact areas was commensurate with the dimension of sub-100 nm tips apexes (Figure 2d). Thereby the photoresist was selectively exposed at sub-100 nm scale areas below the tips apexes. By controlling the exposure dosage, the smallest photoresist line width of 70 nm and the smallest Cr line width of 80 nm were produced respectively (Figure 2g and j). The metal nanopatterns were obtained by metal evaporation on photoresist surface and subsequent photoresist lift off. The obtained sub-wavelength positive photoresist trenches exhibited vertical sidewalls, which could facilitate the transfer of photoresist nanopatterns to other materials conveniently (Figure 2i and Figure S2).[53] Variously shaped nanostructures, including straight line, dot, ladder, circle and branch, were created with sub-wavelength line width or dot diameter by exploiting 20 nm Au coated V-shape PDMS tip array with corresponding horizontal feature shapes as photomasks (Figure 2 and Figure S3).

Journal of Materials Chemistry C Accepted Manuscript

Journal of Materials Chemistry C Accepted Manuscript

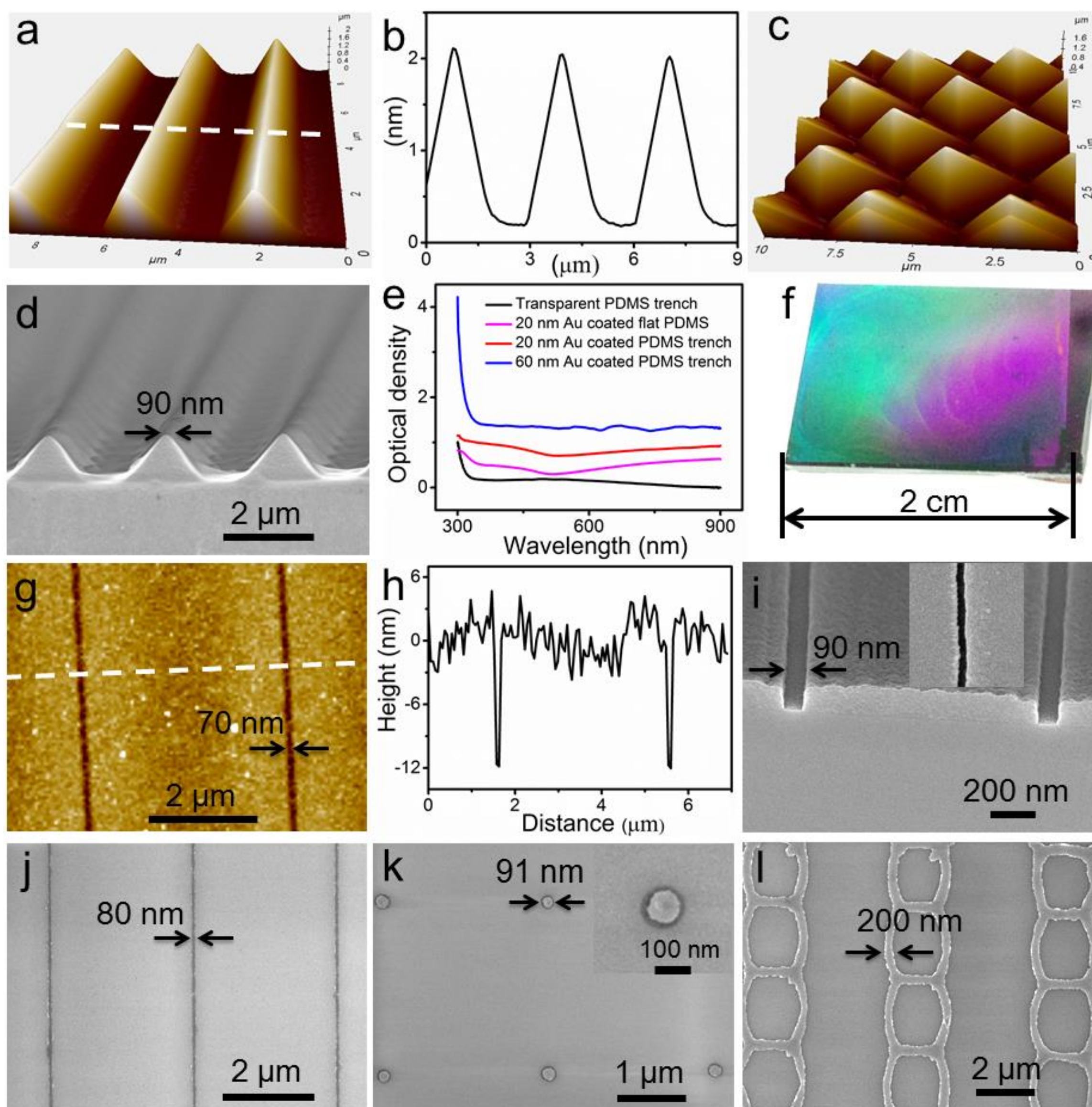

Figure 2. Sub-wavelength photolithography with 20 nm Au coated V-shape PDMS tips without apertures. (a) 3D AFM topographical image of V-shape straight PDMS tip array. (b) AFM height profile of the white line across the tips in (a) revealed the V-shape cross-sectional profile of PDMS tips. (c) 3D AFM topographical image of pyramidal PDMS tips. (d) SEM cross-sectional image of PDMS pyramidal tips with 90 nm apexes. (e) Optical density as a function of wavelength for the PDMS reliefs with different architectures. (f) Optical image of produced sub-wavelength positive photoresist nanopatterns covering the areas of 2×1.5 cm^2. (g-h) AFM

topographical image of positive photoresist trenches with the line width of 70 nm. (i) SEM cross-sectional image of produced positive photoresist trenches with vertical sidewalls. Inset: top-down SEM image of a photoresist trench. (j) SEM image of 80 nm wide Cr lines produced by the photomask in (a). (k) and (l) SEM images of sub-wavelength gold dot and ladder arrays respectively produced using correspondingly shaped PDMS tip arrays as masks.

Investigation of the Effects of Metal Coating Thickness, Tip Apex Size and Exposure Dose on Produced Photoresist Nanopatterns

Appropriate thickness of metal coating on PDMS tip array is essential for achieving the best results. Thus, the effect of Au coating thickness on the morphology of produced positive photoresist nanopatterns was studied (Figure 3). It was found that the incident light could pass from the flat backing parts between V-shape PDMS tips to expose underlying photoresist significantly if no opaque metal or 10 nm thick Au was coated on tips (Figure 3a-b). This made these PDMS tips based photomasks too sensitive to exposure dose and therefore they were not convenient to be used for production of sub-wavelength recessed photoresist nanostructures in this case. For V-shape PDMS tips with thick metal coating such as 60 nm Au, although they could be used to generate 100 nm nanostructures at small areas, massively parallel fabrication of uniform nanopatterns across large areas was difficult if no external pressure was applied on the PDMS photomasks (Figure S4). This was because the inherently adhesive merit of PDMS structures was lost due to the block of thick metal coating. Hence, only the photoresist below the intimate contacted areas could be completely exposed. The photoresist at the areas with gap existed between metal-coated tip apexes and underlying photoresist was only partially exposed (Figure S4e-f). Since 20 nm thick gold coated PDMS tips could achieve the best lithographic

Journal of Materials Chemistry C Accepted Manuscript

results (both small feature size and large patterned areas), they were chosen as adhesive photomasks in this work (Figure 2 and 3c).

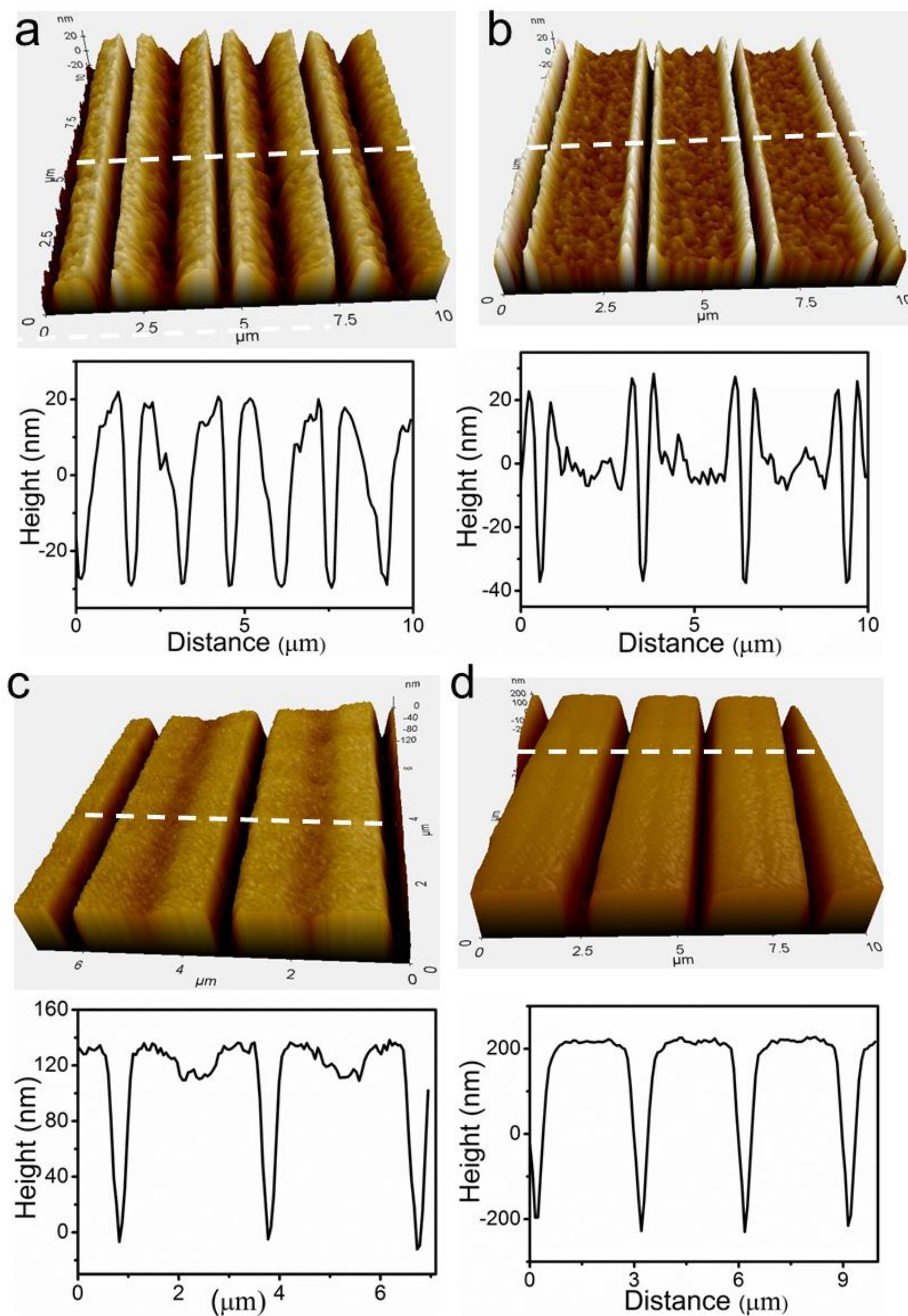

Figure 3. Comparison between V-shape PDMS tip arrays with different thicknesses of Au coating in sub-wavelength photolithography. (a, b, c and d) 3D AFM topographical images of

Journal of Materials Chemistry C Accepted Manuscript

positive photoresist structures produced using V-shape PDMS tip arrays with Au coating thicknesses of 0, 10, 20 and 60 nm respectively as photomasks.

We hypothesized that the PDMS tip apex size was the key factor to dictate the produced feature size since the contact areas were selectively exposed in this approach. By investigating the relationship between tip apex size and correspondingly produced feature size, we found that the produced Cr line width increased nearly linearly with the PDMS tip apex size for the 20 nm Au coated PDMS tips (Figure 4a-e). Besides the tip apex size, the exposure dose was also a important factor to determine produced feature size (Figure 4f-i). The prolonged exposure time resulted in increased feature size apparently. It indicated that the feature size could be programmed by adjusting V-shape PDMS tip apex size and exposure dose. Besides production of sub-wavelength recessed positive photoresist trenches, this lithographic strategy also enabled the fabrication of sub-wavelength raised negative photoresist SU-8 nanopatterns with controllable feature height over large areas (Figure S5).

Journal of Materials Chemistry C Accepted Manuscript

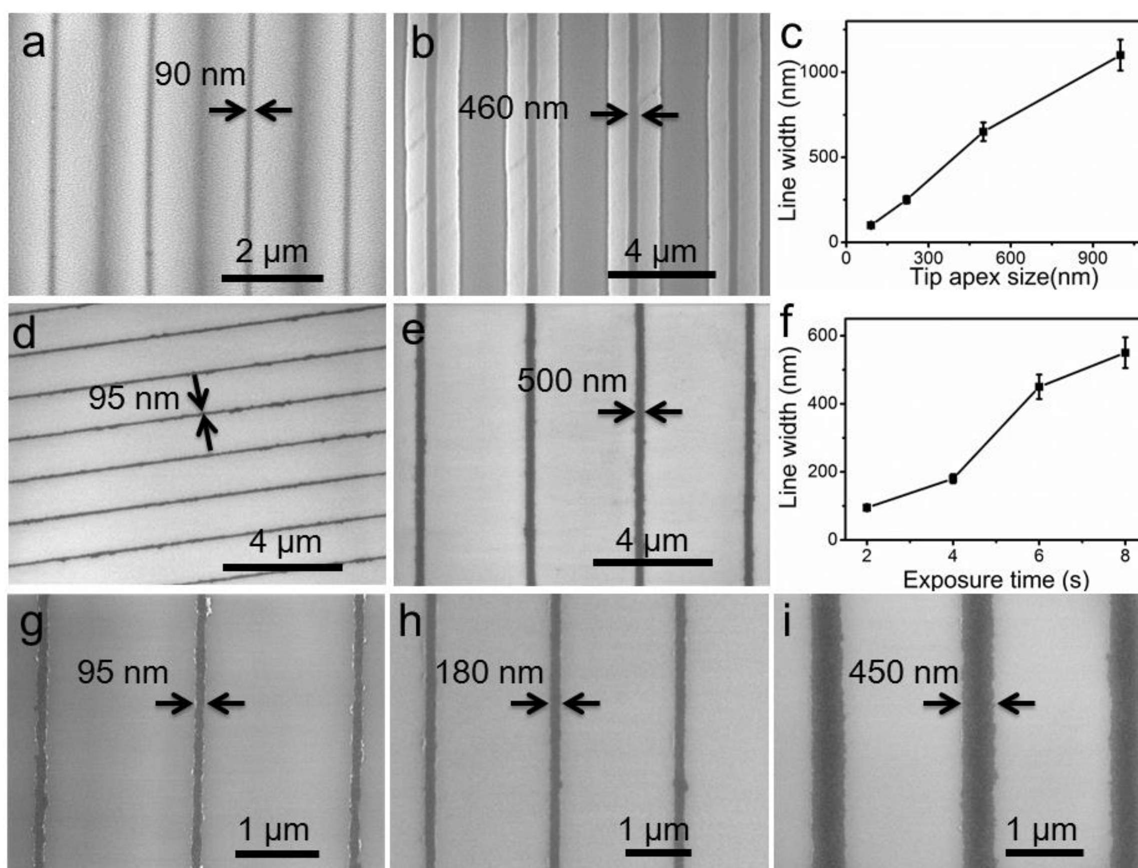

Figure 4. Investigation of the influence of tip apex size and exposure dose on produced feature size. (a) and (b) SEM images of 20 nm Au coated V-shape straight PDMS tip arrays with the apexes widths of 90 and 460 nm respectively. (c) Plot of produced Cr line width as a function of PDMS tip apex size. (d) and (e) SEM images of Cr lines with the line widths of 95 and 500 nm respectively, which were made via the PDMS photomasks in (a) and (b) respectively. (f) Plot of produced Cr line width as a function of exposure time when the same PDMS tip array in (a) was employed as photomask. (g, h and i) SEM images of Cr lines with the line widths of 95, 180 and 450 nm respectively, which were produced by utilizing the exposure time of 2, 4 and 6 s respectively.

Sub-Wavelength Photolithography With Metal Coated V-Shape PDMS Tip Array with Large Apertures

Journal of Materials Chemistry C Accepted Manuscript

Previously, the thick metal coated PDMS tip array with nanoscopic apertures has been utilized to produce sub-wavelength nanostructures.[1, 8] Since the incident light through path 2) is difficult to pass directly from the oblique sidewalls of transparent PDMS tips owing to the total internal reflection effect,[11, 14, 15] in principle, the produced feature size is not sensitive to aperture size at the end of metal-coated V-shape PDMS tips in some degree. Thus, sub-wavelength nanopatterns were also enabled by metal coated PDMS tip array with large apertures at the end of tips in this work (Figure 5). The large apertures made pristine and adhesive PDMS rather than metal at tip apexes contact with underlying photoresist directly. Thus, the intimate contact between tip apex and underlying photoresist surface happened across large areas. The utilization of large apertures substantially simplified the photomasks fabrication process compared with the nanoscopic apertures previously reported.[1, 8] Because the construction of micro-sized apertures was less sensitive to experimental condition variation compared with the creation of nanoscopic apertures, the former was much easier to fabricate than the latter.[28] To study the impact of aperture dimension on the produced feature size, we created the apertures with different aperture widths, such as 90 nm, 300 nm and 1.9 μm at the apexes of 60 nm Au coated V-shape PDMS tips, and investigated their lithographic performance (Figure 5). We chose to coat 60 nm thick Au layer on PDMS tips surface because 60 nm thick Au could block the transmission of incident light from the flat backing parts better than 20 nm thick Au. It was found that the produced metal line width did not increased remarkably with the increment of aperture size. For example, the V-shape PDMS tips with the aperture widths of 90 nm and 1.9 μm produced the photoresist line widths of 97 and 115 nm respectively. Importantly, the photomask with 1.9 μm wide aperture could stick to underlying photoresist coated substrates firmly, whereas the photomasks with 90 and 300 nm wide apertures could not. For the PDMS photomasks with nanoscale apertures, the metal coating

Journal of Materials Chemistry C Accepted Manuscript

at the end of tips may block the intimate contact between PDMS and underlying resist in some degree. This phenomenon was also consolidated by dot apertures created at 60 nm Au coated pyramidal PDMS tips (Figure S6). To make a comparison between thin metal coated V-shape PDMS tips (Figure 1a) and metal-coated V-shape PDMS tips with large apertures (Figure 1b) in producing the smallest feature size, it was found that the latter produced a little larger feature size (Figure 2g and Figure 5d). This may be ascribed to the light propagation through the surrounding areas of transparent tips apexes for the metal-coated tip array with large apertures.[28]

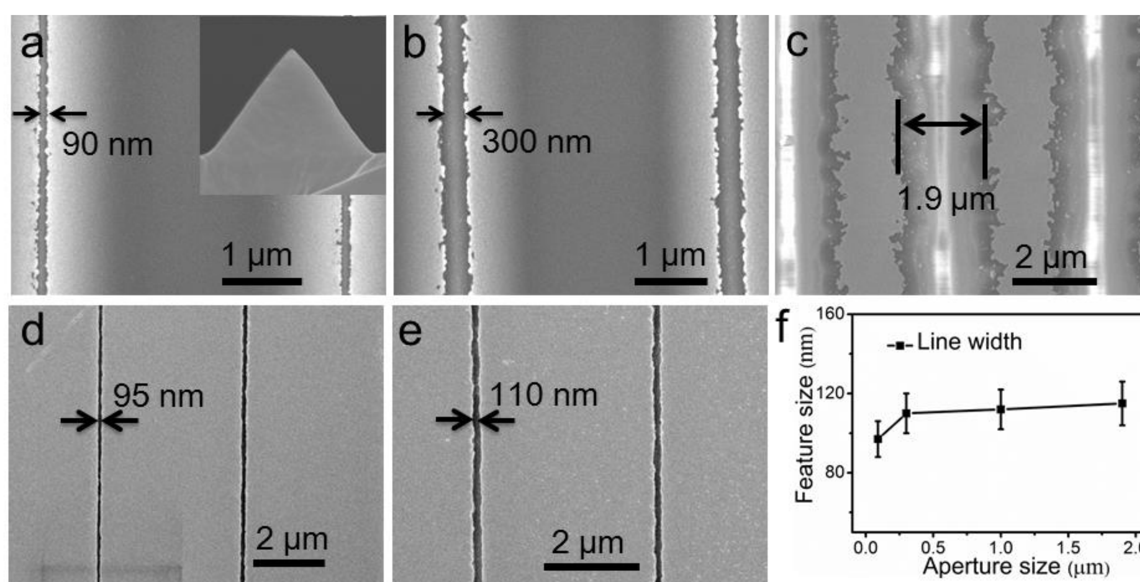

Figure 5. Employing metal-coated V-shape PDMS tips with microscale apertures for sub-wavelength photolithography. (a, b and c) SEM top-down images of 60 nm Au coated V-shape PDMS tips with 90 nm, 300 nm and 1.9 μm wide line apertures respectively created at the end of tips. Inset of (a): SEM cross-sectional image of a V-shape PDMS tip. (d) and (e) SEM top-down images of positive photoresist lines with the line widths of 95 and 110 nm respectively, which were made using the photomasks in (a) and (b) respectively. (f) Plot of generated photoresist line width as a function of tip aperture width.

Journal of Materials Chemistry C Accepted Manuscript

Utilization of Twice Under Exposures to Produce Nanorod Array with Programmable Ratio of Length to Width

Interestingly, it was found that sub-wavelength grid and rod nanopatterns with programmable feature shape and size could be created by rotating the adhesive photomasks in the second of two exposures with controlled exposure energy. On the one hand, the nanorod array with adjustable ratio of length to width could be constructed by employing medium exposure dose (Exposure energy: 105 mW/cm^2, exposure time: 2 s) in two under exposures (Figure 6 and Table. S1). The length of nanorod divided by the width of nanorod was defined as the ratio of length to width. In this case, the exposure dose in the first UV exposure was too low to expose underlying photoresist completely, leading to the formation of photoresist trenches with the depth of 75 nm (Figure 6a-b). The photoresist inside the trenches was not completely removed after the first exposure and development of 130 nm thick positive photoresist coated Si wafers. However, the second UV exposure with the rotation angles of 90 degrees relative to the first exposure made the photoresist at the overlapped areas be selectively exposed completely due to the enhanced exposure dose in two exposures. Hence, the photoresist dot array with the depth of 130 nm formed at the overlapped areas (Figure 6a and c). After metal evaporation on photoresist patterns and subsequent photoresist lift off, only the metal at the overlapped areas was left. Significantly, the shapes of nanodot or nanorod could be adjusted by controlling the rotation angles (Figure 6d-i). For instance, if the rotation angle was 90 degrees, 105 nm round metal dot array could be produced (Figure 6d). However, if the rotation angles were other than 90 degrees, nanorod array formed since the overlapped areas were nanorods (Figure 6e-h). Interestingly, the ratio of length to width of nanorods could be programmed by controlling the rotation angles (Figure 6d-i). For example, when the rotation angles decreased monotonously from 63 to 3 degrees, the ratio of

Journal of Materials Chemistry C Accepted Manuscript

length to width for the nanorod increased from 1.5 to 50 (Figure 6i and Table S1). The metal nanorod array may find application in optics, such as surface plasmonic resonance.[54, 55]

On the other hand, large-area grid nanopatterns with sub-wavelength line width could be obtained if the incident light with high exposure energy (250 mW/cm^2) was employed to fully expose underlying photoresist in single exposure (Figure S7-8). In this case, the shapes and edge lengths of achieved grid nanopatterns could be adjusted conveniently by changing the rotation angles in the second exposure. For example, the grid nanopatterns with square and prism shapes were obtained by rotating the adhesive photomask for 90 and 45 degrees respectively (Figure S7d-i). The edge length of obtained metal grid increased monotonously with the decrease of rotation angles (Figure S8). It demonstrated that sub-wavelength nanopatterns with diversified and programmable feature shapes could be constructed by exploiting two exposures with controlled exposure dosage.

Journal of Materials Chemistry C Accepted Manuscript

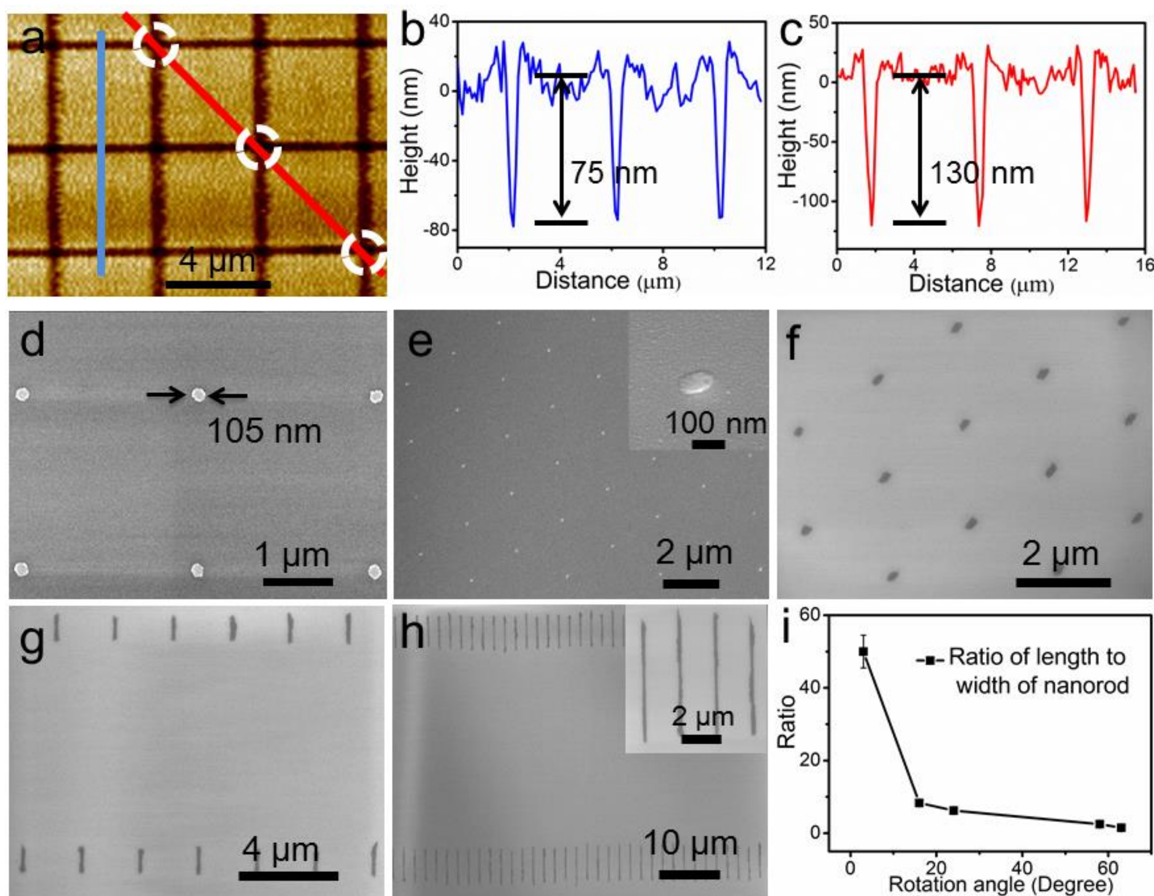

Figure 6. Fabrication of nanoscale rod array by rotating the adhesive V-shape PDMS tip array in two under exposures. (a) AFM topographical image of grid positive photoresist nanopatterns fabricated via two under exposures. (b) AFM height profile of the blue line across the photoresist patterns in (a) demonstrating that the first exposure produced 75 nm high photoresist trenches. (c) AFM height profile of the red line across the overlapped exposed areas in (a) demonstrating that two exposures resulted in 130 nm high photoresist dots at the crossing areas (white circles in (a)). (d) and (e) SEM images of Au dot array and rod array respectively fabricated using the rotation angles of 90 and 63 degrees respectively. (f, g and h) SEM images of Cr nanorod array with different ratios of length to width made by using rotation angles of 58, 16 and 3 degrees respectively. (i) Plot of the ratio of length to width of obtained nanorod as a function of rotation angles.

Journal of Materials Chemistry C Accepted Manuscript

Sub-Wavelength Photolithography by Exploiting Thin Metal Coated PDMS Flat Reliefs as Mask

Similar to the thin metal coated V-shape PDMS tips as explored above, the thin metal coated PDMS flat reliefs also preserved the adhesive characteristic of PDMS, which made them as phase shift photomasks to produce sub-wavelength nanostructures below the sidewalls of PDMS reliefs (Figure 1c and Figure 7a-g).[11, 18, 47, 50] Compared with thin metal coated PDMS flat reliefs, there was difficulty in controlling the exposure dose by employing the transparent PDMS flat reliefs as photomasks to produce sub-wavelength recessed photoresist nanostructures below the sidewalls. For example, all the photoresist at the contact areas between PDMS reliefs and underlying photoresist could be easily exposed if the exposure energy increased a little (> 50 mW/cm^2) (Figure 7h-i), while low exposure energy (< 40 mW/cm^2) could not lead to complete exposure of photoresist below the sidewalls. In contrast, it was found that the photoresist below the edges of PDMS reliefs could be selectively exposed by employing 20 nm thick Au coated PDMS flat reliefs as photomask with a wide range of exposure energy from 45 to 150 mW/cm^2 (Figure 7a-e). Neither the photoresist below the flat protrution of PDMS reliefs nor that below the flat backing parts was exposed significantly, and only the photoresist at nanoscale areas below the sidewalls was completely exposed (Figure 7b-c). Variously shaped two line positive photoresist trenches and the corresponding metal lines with the line width as small as 120 nm were produced in this manner (Figure 7a-g).

Journal of Materials Chemistry C Accepted Manuscript

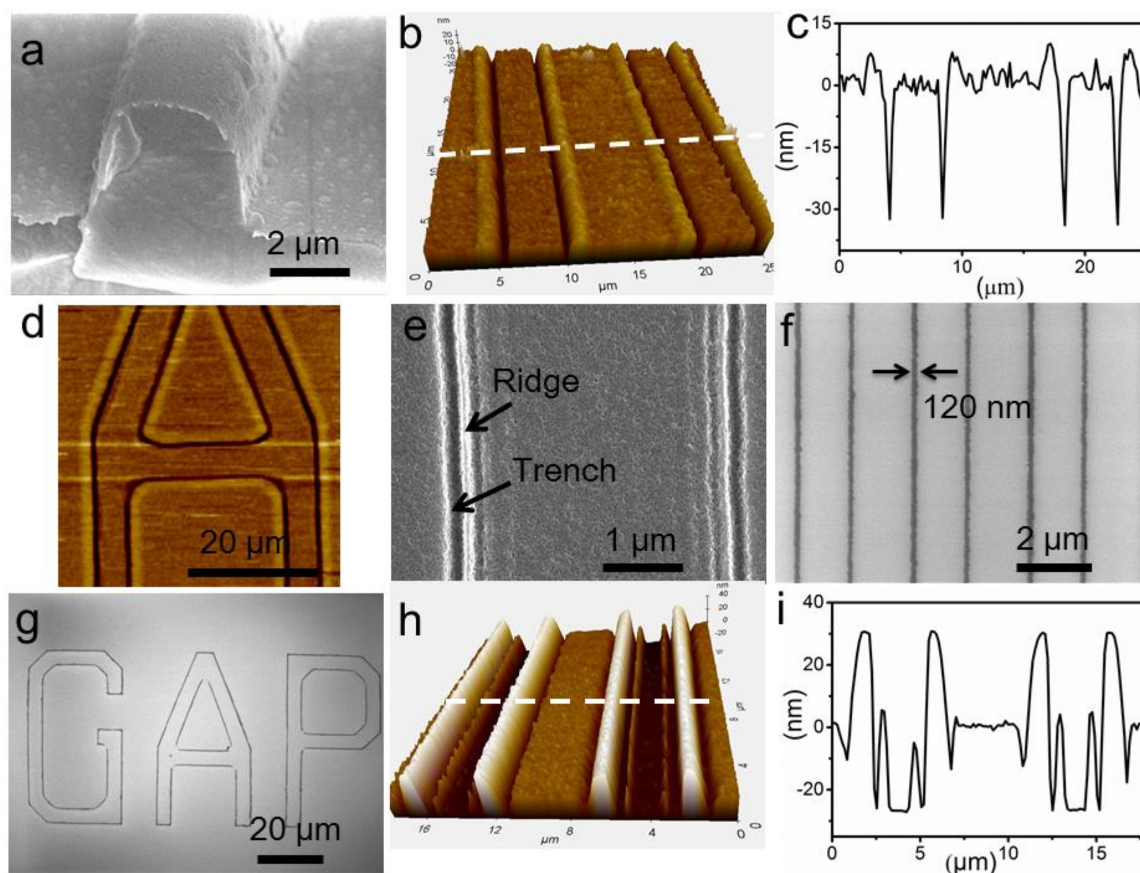

Figure 7. Comparison between thin metal coated PDMS flat reliefs (a-g) and corresponding transparent PDMS flat reliefs (h-i) in near-field photolithography. (a) SEM tilted image of 20 nm Au coated PDMS flat reliefs. (b) 3D AFM topographical image of two-line positive photoresist trench nanostructures made by 20 nm Au coated PDMS flat reliefs. (c) AFM height profile of the white line in (b) across the nanopatterns revealed the recessed trench morphology of the nanopatterns. (d) AFM topographical image of recessed positive photoresist nanopatterns with the shape of letter "A". (e) SEM image of positive photoresist nanopatterns demonstrated that both recessed trenches and raised ridges appeared below the sidewalls of PDMS reliefs due to phase shift effect. (f and g) SEM images of Cr nanopatterns with the shapes of straight two lines and miniaturized letters of "GAP" respectively. (h) 3D AFM image of positive photoresist nanopatterns fabricated by transparent PDMS flat reliefs. (i) AFM height profile of the white line

Journal of Materials Chemistry C Accepted Manuscript

across the structures in (h) suggested that both the photoresist below the sidewalls and that at the contacted areas were exposed.

Production of Sub-Wavelength Molecular Nanopatterns

The integration of bottom-up self-assembled monolayers and top-down (lithographical) is a significant methodology to construct functional nanostructures.[56, 57] Self-assembled monolayers (SAMs) formed on noble metal thin film surface have gained broad interest in nanotechnology community in recent years.[31, 57, 58] One of applications of SAMs is micro/nanofabrication, as in the cases of molecular printing and soft lithography, in which SAMs are employed as resist materials for the production of micro/nanoscale metallic structures in a simple and low-cost manner.[27, 31, 42, 56-58] In this study, with the application of this near-field photolithography strategy, large-area sub-wavelength molecular nanostructures were created on SAMs, opening up the opportunity of light-directed synthesis at nanoscale (Figure 8). Specifically, after immersing 20 nm thick Au coated Si substrate in the solution of dodecanethiol ($HS(CH_2)_{11}CH_3$), SAMs were formed on gold substrates. After the 20 nm Au coated V-shape PDMS tip array was placed on SAMs coated gold substrate and implementation of UV exposure for certain time, the SAMs at the contacted areas between tips apexes and substrate surface were selectively exposed and oxidized, producing nanoscale molecular nanopatterns, as shown in AFM phase images (Figure 8). It was found that the exposure dose was essential to dictate the morphology and size of produced molecular nanostructures. For example, when the exposure time was 1 and 5 min, the produced lines were not continuous, indication of incomplete oxidation (Figure 8a-b). Nevertheless, as the exposure time was prolonged to 10 min, 290 nm wide continuous lines were formed (Figure 8c). As the exposure time was further increased to 20 min, 390 nm wide continuous lines were produced (Figure 8d). In the exposure process, alkanethiolates formed by

Journal of Materials Chemistry C Accepted Manuscript

the adsorption of alkanethiols were oxidized in the presence of air to alkylsulfonates at the contacted areas, leading to the generation of molecular nanopatterns.[59] In future work, the SAMs nanopatterns could be transferred to sub-wavelength functional metal nanostructures via selective metal etching.[57, 58]

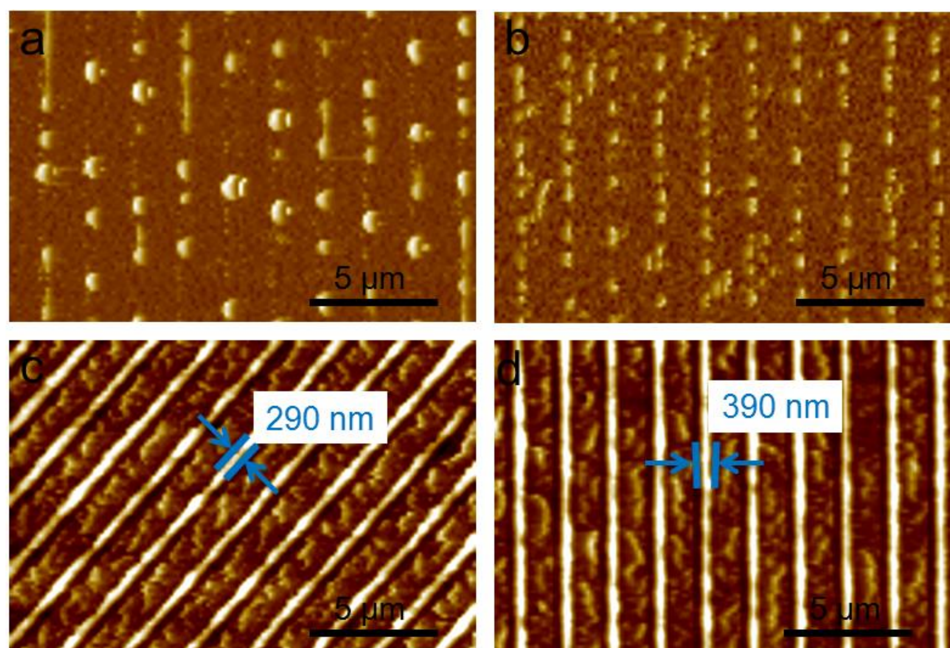

Figure 8. (a, b, c and d) AFM non-contact phase images showing lines created on SAMs of dodecanethiol by 20 nm Au coated V-shape PDMS tips with the exposure time of 1, 5, 10 and 20 min respectively.

To make a comparison between the three kinds of PDMS adhesive photomasks discussed above, the thin metal coated V-shape PDMS tip array without apertures was easiest to fabricate and enabled the smallest feature size (70 nm in line width) (Figure 1a). The metal-coated V-shape PDMS tip array with microscale apertures exhibited the best adhesion behavior because of pristine PDMS at contact areas (Figure 1b). The thin metal coated PDMS flat reliefs generated two line nanopatterns (Figure 1c), instead of one line nanopatterns produced by V-shape PDMS tips. Recently, transparent PDMS based colloidal phase masks have been utilized to fabricate

Journal of Materials Chemistry C Accepted Manuscript

sub-wavelength nanopatterns with high feature density.[60,61] Besides the sub-wavelength 2D nanostructures, the phase shift masks also enable 3D hierarchical architectures composed of alternating array layers.[60,61] Compared with the colloidal phase masks, our reported adhesive photomasks provides long range highly ordered nanopatterns with diversified feature geometries since the elastomeric masks are fabricated from traditional top-down photolithography. In contrast, colloidal phase masks gain the advantages of offering sub-wavelength feature periodicity and programmable dimensions of nanostructures, e.g, 2D and 3D nanostructures. The advantage of this technique is that hundreds of PDMS replicas can be produced from one single mold repeatedly, demonstrating the low-cost merit of this strategy. The drawback of this strategy is the microscale periodicity of produced nanopatterns currently, which is determined by initial chrome photomasks in traditional photolithography. In future work, the density of nanopatterns could be increased by utilizing other high resolution lithographic methods to fabricate the silicon molds, such as EBL and nanoimprint lithography.[21, 22]

Conclusions

In summary, sub-wavelength nanopatterns with variable feature shapes over centimeter-scale areas were fabricated by utilizing metal coated adhesive PDMS structures as photomasks. The metal coating with controlled thickness enables the manipulation of incident light path, allowing nanoscale areas below the V-shape PDMS tips apexes or the sidewalls of PDMS flat reliefs to be selectively exposed. Thanks to the adhesive merit of PDMS, the elastomeric photomasks could contact with underlying photoresist intimately, leading to the formation of sub-wavelength nanostructures over large areas. For the firt time, a new method was developed to fabricate nanorod array with programmable ratio of length to width by rotating the adhesive photomasks

Journal of Materials Chemistry C Accepted Manuscript

in two exposures with controlled exposure dose, indication of the flexibility of this technique. Besides production of the smallest feature size of 70 nm on photoresist surface, this nanolithography strategy also enabled large-area other nanopatterns, such as sub-wavelength molecular nanopatterns, suggesting the versatility of this technique. It was found that the metal coating thickness, PDMS tip apex size and exposure dose played important roles in dictating the size and uniformity of produced nanopatterns. Because this lithographic strategy offers the merits of high throughput, low cost, flexible feature size, shape and composition, it provides new opportunity to produce functional nanostructures for relevant academic applications in future work, such as transparent electrodes, plasmonics and cell matrix adhesion formation and migration study.[12, 48, 62]

Associated content

Supporting Information Available: Investigation of the influence of exposure dose on the morphology of produced positive photoresist structures, variously shaped positive photoresist nanopatterns produced by employing V-shape PDMS tips with 20 and 60 nm thick Au coating respectively, production of sub-wavelength raised negative photoresist SU-8 nanopatterns, study the effect of aperture size at metal-coated pyramidal PDMS tip apexes on the produced metal dot size, the dependence of the ratio of length to width of produced nanorod on the rotation angle of masks in the second UV exposure, fabrication of large-area grid and prism shaped positive photoresist nanopatterns by rotating the photomasks in two exposures.

References

1. X. Liao, K. A. Brown, A. L. Schmucker, G. Liu, S. He, W. Shim and C. A. Mirkin, *Nat. Commun.* 2013, **4**, 2103.

Journal of Materials Chemistry C Accepted Manuscript

2. L. Persano, A. Camposeo and D. Pisignano, *J. Mater. Chem. C* 2013, **1**, 7663-7680.

3. J. Wu, X. L. Zan, S. Z. Li, Y. Y. Liu, C. L. Cui, B. H. Zou, W. N. Zhang, H. B. Xu, H. W. Duan, D. B. Tian, W. Huang and F. W. Huo, *Nanoscale* 2014, **6**, 749-752.

4. J. Wu, C. H. Yu, S. Z. Li, B. H. Zou, Y. Y. Liu, X. Q. Zhu, Y. Y. Guo, H. B. Xu, W. N. Zhang, L. P. Zhang, B. Liu, D. B. Tian, W. Huang, M. P. Sheetz and F. W. Huo, *Langmuir* 2015, **31**, 1210-1217.

5. C. D. O'Connell, M. J. Higgins, S. E. Moulton and G. G. Wallace, *J. Mater. Chem. C,* 2015. DOI: 10.1039/C5TC00186B

6. B. Schumm, F. M. Wisser, G. Mondin, F. Hippauf, J. Fritsch, J. Grothe and S. Kaskel, *J. Mater. Chem. C*, 2013, **1**, 638-645.

7. J. Li, W. Gao, R. Dong, A. Pei, S. Sattayasamitsathit and J. Wang, *Nat. Commun.* 2014, **5**, 5026.

8. F. W. Huo, G. F. Zheng, X. Liao, L. R. Giam, J. A. Chai, X. D. Chen, W. Y. Shim and C. A. Mirkin, *Nat. Nanotechnol*. 2010, **5**, 637-640.

9. J. Wu and J. M. Miao, *ACS Appl. Mater. Interfaces* 2015, **7**, 6991-7000.

10. J. Wu, Y. Y. Liu, Y. Y. Guo, S. L. Feng, B. H. Zou, H. Mao, C. H. Yu, D. B. Tian, W. Huang and F. W. Huo, *Langmuir* 2015, **31**, 5005−5013.

11. T. W. Lee, S. Jeon, J. Maria, J. Zaumseil, J. W. P. Hsu and J. A. Rogers, *Adv. Funct. Mater*. 2005, **15**, 1435-1439.

12. J. G. Ok, M. K. Kwak, C. M. Huard, H. S. Youn and L. J. Guo, *Adv.Mater.* 2013, **25**, 6554-6561.

13. X. C. Zhou, Z. L. Liu, Z. Xie, X. Q. Liu and Z. J. Zheng, *Small* 2012, **8**, 3568-3572.

14. D. Qin, Y. N. Xia, A. J. Black and G. M. Whitesides, *J. Vac. Sci. Technol., B* 1998, **16**, 98-

Journal of Materials Chemistry C Accepted Manuscript

103.

15. A. M. Bowen, M. J. Motala, J. M. Lucas, S. Gupta, A. J. Baca, A. Mihi, A. P. Alivisatos, P. V. Braun and R. G. Nuzzo, *Adv. Funct. Mater*. 2012, **22**, 2927-2938.
16. S. C. Laza, M. Polo, A. A. Neves, R. Cingolani, A. Camposeo and D. Pisignano, *Adv. Mater.* 2012, **24**, 1304-1308.
17. W. Srituravanich, L. Pan, Y. Wang, C. Sun, D. B. Bogy and X. Zhang, *Nat. Nanotechnol*. 2008, **3**, 733-737.
18. J. A. Rogers; K. E. Paul; R. J. Jackman; G. M. Whitesides, *J. Vac. Sci. Technol., B* 1998, **16**, 59-68.
19. S. D. Bian, S. B. Zieba, W. Morris, X. Han, D. C. Richter, K. A. Brown, C. A. Mirkin and A. B. Braunschweig, *Chem. Sci.* 2014, **5**, 2023-2030.
20. A. J. Storm, J. H. Chen, X. S. Ling, H. W. Zandbergen and C. Dekker, *Nat. Mater.* 2003, **2**, 537-540.
21. K. Hoflich, R. B. Yang, A. Berger, G. Leuchs and S. Christiansen, *Adv. Mater.* 2011, **23**, 2657-2661.
22. G. Kumar, H. X. Tang and J. Schroers, *Nature* 2009, **457**, 868-872.
23. H. B. Lan, Y. C. Ding, H. Z. Liu and B. H. Lu, *Microelectron. Eng.* 2007, **84**, 684-688.
24. S. Kramer, R. R. Fuierer and C. B. Gorman, *Chem. Rev.* 2003, **103**, 4367-4418.
25. W. Shim, A. B. Braunschweig, X. Liao, J. Chai, J. K. Lim, G. Zheng and C. A. Mirkin, *Nature* 2011, **469**, 516-520.
26. K. Salaita, Y. H. Wang and C. A. Mirkin, *Nat. Nanotechnol*. 2007, **2**, 145-155.
27. F. W. Huo, Z. J. Zheng, G. Zheng, L. R. Giam, H. Zhang and C. A. Mirkin, *Science* 2008, **321**, 1658-1660.

Journal of Materials Chemistry C Accepted Manuscript

28. Y. Zhou, Z. Xie, K. A. Brown, D. J. Park, X. Z. Zhou, P. C. Chen, M. Hirtz, Q. Y. Lin, V. P. Dravid, G. C. Schatz, Z. J. Zheng and C. A. Mirkin, *Small* 2014, **11**, 913-918.
29. S. Kim, B. Marelli, M. A. Brenckle, A. N. Mitropoulos, E. S. Gil, K. Tsioris, H. Tao, D. L. Kaplan and F. G. Omenetto, *Nat. Nanotechnol*. 2014, **9**, 306-310.
30. J. W. Jang, B. Park and S. Nettikadan, *Nanoscale* 2014, **6**, 7912-7916.
31. D. J. Eichelsdoerfer, X. Liao, M. D. Cabezas, W. Morris, B. Radha, K. A. Brown, L. R. Giam, A. B. Braunschweig and C. A. Mirkin, *Nat. Protoc*. 2013, **8**, 2548-2560.
32. C. B. Tang, E. M. Lennon, G. H. Fredrickson, E. J. Kramer and C. J. Hawker, *Science* 2008, **322**, 429-432.
33. J. A. Chai, F. W. Huo, Z. J. Zheng, L. R. Giam, W. Shim and C. A. Mirkin, *Proc. Natl. Acad. Sci. U. S. A.* 2010, **107**, 20202-20206.
34. P. Jiang and M. J. McFarland, *J. Am. Chem. Soc.* 2005, **127**, 3710-3711.
35. C. H. Chang, L. Tian, W. R. Hesse, H. Gao, H. J. Choi, J. G. Kim, M. Siddiqui and G. Barbastathis, *Nano Lett*. 2011, **11**, 2533-2537.
36. S. Huang, H. Zhang, Z. Wu, D. Kong, D. Lin, Y. Fan, X. Yang, Z. Zhong, S. Huang, Z. Jiang and C. Cheng, *ACS Appl. Mater. Interfaces* 2014, **6**, 12111-12118.
37. X. Li, H. Tian, C. Wang, X. Li, J. Shao, Y. Ding and L. Wang, *ACS Appl. Mater. Interfaces* 2014, **6**, 12737-12743.
38. X. Li, H. Tian, J. Shao, Y. Ding and H. Liu, *Langmuir* 2013, **29**, 1351-1355.
39. E. Schaffer, T. Thurn-Albrecht, T. P. Russell and U. Steiner, *Nature* 2000, **403**, 874-877.
40. N. Wu and W. B. Russel, *Nano Today* 2009, **4**, 180-192.
41. J. A. Liddle and G. M. Gallatin, *Nanoscale* 2011, **3**, 2679-2688.
42. M. Geissler and Y. N. Xia, *Adv. Mater.* 2004, **16**, 1249-1269.

Journal of Materials Chemistry C Accepted Manuscript

43. H. Schmid, H. Biebuyck, B. Michel and O. J. F. Martin, *Appl. Phys. Lett*. 1998, **72**, 2379-2381.

44. A. d. Campo and C. Greiner, *J. Micromech. Microeng.* 2007, **17**, R81-R95.

45. J. Maria, V. Malyarchuk, J. White and J. A. Rogers, *J. Vac. Sci. Technol., B* 2006, **24**, 828-835.

46. C. Y. Wu and Y. C. Lee, *Opt. Express* 2014, **22**, 10593-10604.

47. J. Henzie, M. H. Lee and T. W. Odom, *Nat. Nanotechnol*. 2007, **2**, 549-554.

48. E. Menard, M. A. Meitl, Y. G. Sun, J. U. Park, D. J. L. Shir, Y. S. Nam, S. Jeon and J. A. Rogers, *Chem. Rev.* 2007, **107**, 1117-1160.

49. H. Hu, J. Yeom, G. Mensing, Y. Chen, M. A. Shannon and W. P. King, *Nanotechnology* 2012, **23**, 175303.

50. T. W. Odom, J. C. Love, D. B. Wolfe, K. E. Paul and G. M. Whitesides, *Langmuir* 2002, **18**, 5314-5320.

51. Z. Wang, R. B. Xing, X. H. Yu and Y. C. Han, *Nanoscale* 2011, **3**, 2663-2678.

52. A. Carlson, A. M. Bowen, Y. Huang, R. G. Nuzzo and J. A. Rogers, *Adv. Mater.* 2012, **24**, 5284-5318.

53. M. D. Huntington and T. W. Odom, *Small* 2011, **7**, 3144-3147.

54. G. Vecchi, V. Giannini and J. Gómez Rivas, *Phys. Rev. Lett.* 2009, **102**, 146807.

55. M. H. Lee, H. Gao, J. Henzie and T. W. Odom, *Small* 2007, **3**, 2029-2033.

56. G. J. Leggett, *Chem. Soc. Rev.* 2006, **35**, 1150-1161.

57. G. J. Leggett, *Nanoscale* 2012, **4**, 1840-1855.

58. R. E. Ducker and G. J. Leggett, *J. Am. Chem. Soc.* 2006, **128**, 392-393.

59. S. Q. Sun, K. S. L. Chong and G. J. Leggett, *J. Am. Chem. Soc.* 2002, **124**, 2414-2415.

Journal of Materials Chemistry C Accepted Manuscript

60. T. Y. Jeon, H. C. Jeon, S. Y. Lee, T. S. Shim, J.-D. Kwon, S.-G. Park, S.-M. Yang, *Adv. Mater.* 2014, **26**, 1422-1426.

61. M. Fang, H. Lin, H. Y. Cheung, S. Yip, F. Xiu, C.-Y. Wong, J. C. Ho, *Adv. Opt. Mater*. 2014, **2**, 855−860.

62. P. M. Nair, K. Salaita, R. S. Petit and J. T. Groves, *Nat. Protoc*. 2011, **6**, 523-539.

Journal of Materials Chemistry C Accepted Manuscript

Journal of Materials Chemistry C Accepted Manuscript

TOC Graphic

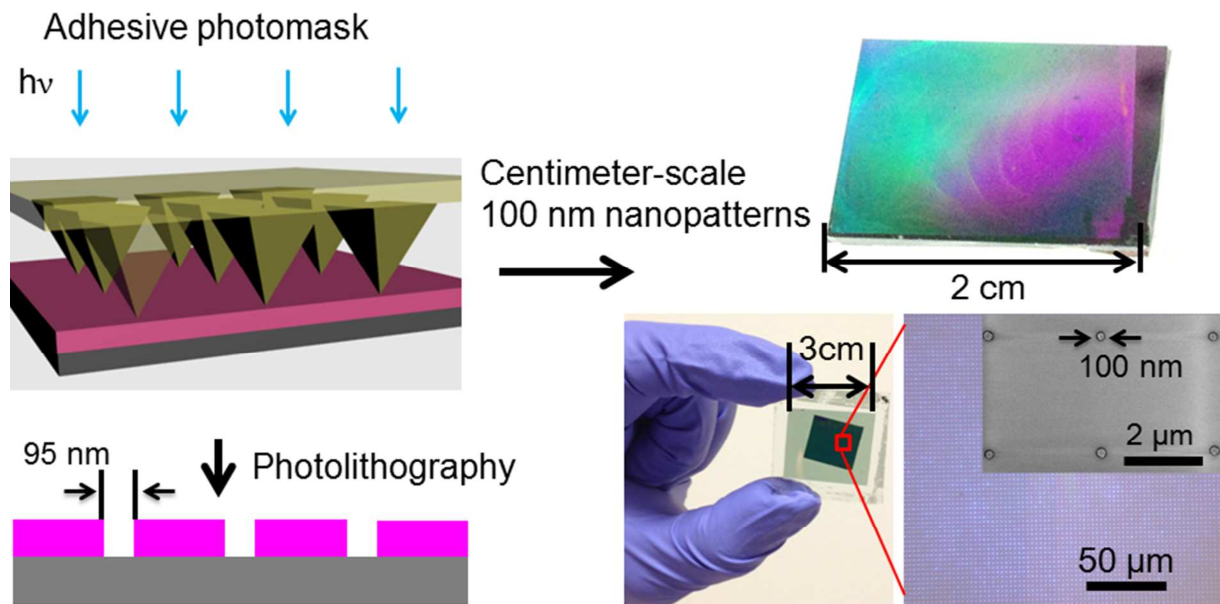

Centimeter-scale sub-wavelength metal and molecular nanopatterns are generated by manipulating the light path of adhesive polymer based photomask.